

Dataset-learning duality and emergent criticality

Ekaterina Kukleva¹ and Vitaly Vanchurin^{1,2}

¹Artificial Neural Computing, Weston, Florida, 33332, USA

²Duluth Institute for Advanced Study, Duluth, Minnesota, 55804, USA

E-mail: ekaterina.kukleva.99@gmail.com, vitaly.vanchurin@gmail.com

Abstract. In artificial neural networks, the activation dynamics of non-trainable variables is strongly coupled to the learning dynamics of trainable variables. During the activation pass, the boundary neurons (e.g., input neurons) are mapped to the bulk neurons (e.g., hidden neurons), and during the learning pass, both bulk and boundary neurons are mapped to changes in trainable variables (e.g., weights and biases). For example, in feed-forward neural networks, forward propagation is the activation pass and backward propagation is the learning pass. We show that a composition of the two maps establishes a duality map between a subspace of non-trainable boundary variables (e.g., dataset) and a tangent subspace of trainable variables (i.e., learning). In general, the dataset-learning duality is a complex non-linear map between high-dimensional spaces, but in a learning equilibrium, the problem can be linearized and reduced to many weakly coupled one-dimensional problems. We use the duality to study the emergence of criticality, or the power-law distributions of fluctuations of the trainable variables. In particular, we show that criticality can emerge in the learning system even from the dataset in a non-critical state, and that the power-law distribution can be modified by changing either the activation function or the loss function.

Contents

1	Introduction	1
2	Neural networks	2
3	Dataset-learning duality	4
4	Jacobian matrix	6
5	Toy model	7
6	Emergent criticality	9
7	Power-law map	10
8	Numerical results	12
8.1	Exponential composition, $k_q = 1$	13
8.2	Quadratic composition, $k_q = 0$	17
8.3	Logarithmic composition, $k_q = -2$	19
9	Fractional powers	21
10	Discussion	24

1 Introduction

Dualities provide a highly useful technique for solving complex problems that have found applications in many branches of science, most notably in physics. For example, well-known dualities include electric-magnetic duality [1], wave-particle duality [2], target-space dualities [3], etc. More recent, but less-known examples include a quantum-classical duality [4], dual path integral [5], and duality pseudo-forest [6], to name a few. The key idea of all physical dualities is to establish a mapping (i.e., a duality mapping) between two systems (e.g., physical theories), which can then be used to study properties (e.g., obtaining solutions) of one system by analyzing the other system, or vice versa.

Perhaps the most well-studied example of a physical duality is the so-called bulk-boundary or holographic duality [7], such as AdS-CFT [8]. In AdS-CFT, the mapping is established between the bulk, representing a gravitational theory on the anti-de Sitter (AdS) background, and the boundary, representing a conformal field theory (CFT) without gravity.

In this article, we shall consider not a physical, but a learning duality, which we shall refer to as the dataset-learning duality. It is often convenient to view the dataset as representing the states of non-trainable variables on the ‘boundary’, and

learning as representing the dynamics (or changes of states) of trainable variables in the ‘bulk’. Thus, the dataset-learning duality may be considered as an example of a bulk-boundary duality in the context of learning theory. As we shall argue, the duality is a complex non-linear mapping between very high-dimensional spaces, but near equilibrium state, the analysis is greatly simplified. This simplification allows us to apply the dataset-learning duality to study the emergence of criticality in learning systems.

Criticality in physical systems refers to the behavior of these systems at or near critical points, where they undergo phase transitions. These critical points are characterized by dramatic changes in physical properties due to the collective behavior of the system’s components. Understanding phase transitions and criticality is essential for explaining many physical phenomena [9] as well as complex biological phenomena such as biological phase transitions [10]. Recent studies have shown that many physical [11–13] and biological [14, 15] systems can be modeled as learning systems, such as artificial neural networks. Therefore, understanding the criticality and phase transitions in artificial neural networks may also shed light on the emergence of criticality in physical and biological systems.

The first step in this direction was made in Ref. [16], where the criticality, or a power-law distribution of fluctuations, was derived analytically using a macroscopic, or thermodynamic, description developed in [17]. This results was then confirmed numerically [16] for a classification learning task involving handwritten digits [18]. In this paper, we take another step towards developing a theory of emergent criticality by providing a more microscopic description of the phenomena using the dataset-learning duality. We then test our predictions numerically for a toy-model classification task.

The paper is organized as follows. In Sec. 2 a theoretical model of neural networks and basic notations are introduced. Sec. 3 is devoted to developing a statistical description of a local dataset-learning duality and in Sec. 4 the Jacobian matrix for the duality mapping is derived. In Sec. 5 a toy-model with two trainable and two non-trainable variables is introduced. In Sec. 6 the toy-model is solved for power-law fluctuations of the trainable variables and in Sec. 7 conditions for criticality are obtained for a power-law mapping. In Sec. 8 we present numerical results for some specific power-law distributions and in Sec. 9 other cases with fractional powers are discussed. In Sec. 10 we summarize and discuss the main results of the paper.

2 Neural networks

Consider an artificial neural network defined as a neural septuple $(\mathbf{x}, \hat{P}, p_{\partial}, \hat{w}, \mathbf{b}, \mathbf{f}, H)$ [17], where:

1. $\mathbf{x} \in \mathbb{R}^N$, is a vector state of N neurons,
2. \hat{P} , is a projection to subspace of $N_{\partial} = \text{Tr}(\hat{P})$ boundary neurons,
3. $p_{\partial}(\mathbf{x}_{\partial})$, is a probability distribution which describes the training dataset,

4. $\hat{w} \in \mathbb{R}^{N^2}$, is a weight matrix which describes connections between neurons,
5. $\mathbf{b} \in \mathbb{R}^N$, is a bias vector which describes bias in inputs of individual neurons,
6. $\mathbf{f}(\hat{w}\mathbf{x}+\mathbf{b})$, is an activation map which describes a non-linear part of the dynamics,
7. $H(\mathbf{x}, \hat{w}, \mathbf{b})$, is a loss function of both trainable and non-trainable variables.

It is assumed that the bias vector \mathbf{b} and weight matrix \hat{w} are the only trainable parameters which can be combined into a single trainable vector,¹

$$\begin{aligned} w_{ij} &= W_{ij}^l q_l = \delta_{i(N-1)+j}^l q_l, \\ b_i &= B_i^l q_l = \delta_{N^2+i}^l q_l. \end{aligned} \quad (2.1)$$

where δ_j^i is the Kronecker delta symbol.

In standard neural networks, including feedforward [19], convolutional [20], auto-encoder [21], transformers [22], etc., certain trainable variables can be shared, fixed, or set to zero, but all such architectures can be described using appropriate choices of constant tensors W_{ij}^l and B_i^l . Then Eq. (2.1) can be viewed as a linear map from K -dimensional space of trainable variables to $N^2 + N$ -dimensional space of weights and biases, where K can be much smaller than $N^2 + N$.

The neural septuple $(\mathbf{x}, \hat{P}, p_\partial, \hat{w}, \mathbf{b}, \mathbf{f}, H)$ defines the three relevant types of dynamics and their relevant time-scales:

- Activation dynamics describes changes of bulk neurons $\mathbf{x}_\partial = \hat{P}\mathbf{x}$ on the smallest time scale which can be set to one,

$$\mathbf{x}_\partial(t+1) = (\hat{I} - \hat{P})\mathbf{x}(t+1) = (\hat{I} - \hat{P})\mathbf{f}(\hat{w}\mathbf{x}(t) + \mathbf{b}). \quad (2.2)$$

- Boundary dynamics describes updates of boundary neurons $\mathbf{x}_\partial = \hat{P}\mathbf{x}$ on the intermediate time-scales, e.g. once per L unit time steps, e.g. drawn from probability distribution $p_\partial(\mathbf{x}_\partial)$ which describes the dataset.
- Learning dynamics describes changes of trainable variables \mathbf{q} on the largest time-scale ML where M is the so-called mini-batch size. For example, for the stochastic gradient descent method,

$$\dot{q}_i = -\gamma \frac{\partial \langle H \rangle_M}{\partial q_i} \quad (2.3)$$

where $\langle \dots \rangle_M$ is the averaging over mini-batch and γ is the learning rate.

In what follows we will be interested in the duality mapping from the boundary space of dimension N_∂ to the K -dimensional tangent space of trainable variables. As we shall see, the map is a composition of the activation and learning passes.

¹Einstein summation convention over repeated indices is implied here and throughout the manuscript unless stated otherwise.

3 Dataset-learning duality

The main objective of this section is to establish a duality mapping between the tangent space of trainable variables and the boundary subspace of non-trainable variables. For starters, we consider a large neural network, defined in Sec. 2, in a local learning equilibrium [17]. In other words, the subject of the study will be a high-dimensional, yet local, problem that allows for significant simplifications. In particular, this allows us to reduce the effective dimensionality K of the space of trainable variables to the dimensionality of the space of non-trainable variables N , or even to the dimensionality of the boundary subspace of non-trainable variables $N_\partial = \text{Tr}(\hat{P})$. However, we will not consider possible symmetries in the dataset that could potentially reduce the dimensionality further.

The learning dynamics, described by Eq. (2.3), can be viewed as a map from non-trainable degrees of freedom \mathbf{x} to changes of trainable degrees of freedom $\dot{\mathbf{q}}$, i.e.

$$\dot{\mathbf{q}} = \dot{\mathbf{q}}(\mathbf{f}, \mathbf{x}_\partial(t_n), \mathbf{x}_\partial(t_{n-1}), \dots, \mathbf{x}_\partial(t_0), \mathbf{x}_\partial | \mathbf{q}). \quad (3.1)$$

For example, if the loss function of trainable and non-trainable variables is separable, i.e.

$$H = H_x(\mathbf{x}) + H_q(\mathbf{q}), \quad (3.2)$$

where

$$\mathbf{x}(t) = (\hat{P}\mathbf{x}(t), (\hat{I} - \hat{P})\mathbf{x}(t)) = (\mathbf{x}_\partial, (\hat{I} - \hat{P})\mathbf{f}(\hat{w}\mathbf{x}(t-1) + \mathbf{b})) = (\mathbf{x}_\partial, \mathbf{x}_\partial(t)), \quad (3.3)$$

then evolution of weights and biases is given by

$$\begin{aligned} \dot{b}_j &= -\gamma \frac{\partial H_q}{\partial b_j} - \gamma f_j' \left(\sum_i w_{ji} x_i(t_{n-1}) + b_j \right) \frac{\partial H_x}{\partial f_j} + \dots, \\ \dot{w}_{jk} &= -\gamma \frac{\partial H_q}{\partial w_{jk}} - \gamma x_k f_j' \left(\sum_i w_{ji} x_i(t_{n-1}) + b_j \right) \frac{\partial H_x}{\partial f_j} + \dots \end{aligned} \quad (3.4)$$

where the mini-batch size is set to $M = 1$. Here f_i' denotes derivative of activation functions with respect to its argument, i.e. describing the first step in back-propagation algorithms, and ellipsis denoting higher order terms.

The activation dynamics, in turn, makes it possible to establish a connection between the initial state of the vector of non-trainable variables $(\mathbf{x}_\partial, \mathbf{x}_\partial(t_0))$ and its state at later time $(\mathbf{x}_\partial, \mathbf{x}_\partial(t_i))$, i.e.

$$\begin{aligned} \mathbf{x}_\partial(t_1) &= \mathbf{f}(\mathbf{x}_\partial(t_0), \mathbf{x}_\partial | \mathbf{q}), \\ \mathbf{x}_\partial(t_2) &= \mathbf{f}(\mathbf{x}_\partial(t_1), \mathbf{x}_\partial | \mathbf{q}), \\ &\dots \\ \mathbf{x}_\partial(t_n) &= \mathbf{f}(\mathbf{x}_\partial(t_{n-1}), \mathbf{x}_\partial | \mathbf{q}) = \mathbf{f}(\mathbf{x}_\partial(t_{n-1}, \mathbf{x}_\partial(t_0), \mathbf{x}_\partial, \mathbf{q}), \mathbf{x}_\partial | \mathbf{q}). \end{aligned} \quad (3.5)$$

where t_0 is the initial time before activation pass and $t_i = t_0 + i$ is time after i steps of activation. Note that during the activation pass, the input neurons \mathbf{x}_∂ remain fixed and act as a source for the bulk neurons $\mathbf{x}_\neq(t_i)$, which change with time t_i .

Composition of the activation (3.5) and learning (3.1) maps is a map from non-trainable degrees of freedom $(\mathbf{x}_\partial, \mathbf{x}_\neq(t_0))$ at time t_0 to changes of trainable degrees of freedom $\dot{\mathbf{q}}$ at time t_n , i.e.

$$(\mathbf{x}_\partial, \mathbf{x}_\neq(t_0)|\mathbf{q}) \rightarrow \dot{\mathbf{q}}. \quad (3.6)$$

For example, if the learning dynamics is described by stochastic gradient descent with mini-batch size $M = 1$, then the map is given by

$$\dot{q}_k(\mathbf{x}_\partial, \mathbf{x}_\neq(t_0)|\mathbf{q}) = -\gamma \left(\frac{\partial f_j}{\partial q^k} \frac{\partial}{\partial f_j} + \frac{\partial}{\partial q^k} \right) H(\mathbf{f}(\mathbf{x}_\neq(t_0), \mathbf{x}_\partial|\mathbf{q}), \mathbf{x}_\partial|\mathbf{q}). \quad (3.7)$$

which is a map from N_∂ -dimensional space of non-trainable boundary variables to K -dimensional space of fluctuations of trainable variables. Therefore the probability distribution $p_{\dot{\mathbf{q}}}(\dot{\mathbf{q}})$ can be expressed as

$$p_{\dot{\mathbf{q}}}(\dot{\mathbf{q}}|\mathbf{q}) = \int p_{x_\partial x_\neq}(\mathbf{x}_\partial, \mathbf{x}_\neq(t_0)) \delta^{(K)}(\dot{\mathbf{q}} - \dot{\mathbf{q}}(\mathbf{x}_\neq(t_0), \mathbf{x}_\partial|\mathbf{q})) d^{N_\partial} x(t_0). \quad (3.8)$$

where the different subscripts are used to emphasize that these are different probability distribution functions, e.g. $p_{\dot{\mathbf{q}}}()$ and $p_{x_\partial x_\neq}()$ (which is also apparent from the arguments of these functions), and the vertical bar is used for conditional distribution, e.g. $p_{\dot{\mathbf{q}}}(\dot{\mathbf{q}}|\mathbf{q})$. If the bulk neurons are initialized to zeros (or other constant values) at t_0 , then $p_{x_\partial x_\neq}(\mathbf{x}_\partial, \mathbf{x}_\neq(t_0)) = p_{x_\partial}(\mathbf{x}_\partial) \delta^{(N_\neq)}(\mathbf{x}_\neq(t_0))$, and by integrating (3.8) over $\mathbf{x}_\neq(t_0)$ we get

$$p_{\dot{\mathbf{q}}}(\dot{\mathbf{q}}|\mathbf{q}) = \int p_{x_\partial}(\mathbf{x}_\partial) \delta^{(K)}(\dot{\mathbf{q}} - \dot{\mathbf{q}}(\mathbf{x}_\partial|\mathbf{x}_\neq(t_0), \mathbf{q})) d^{N_\partial} x_\partial. \quad (3.9)$$

Note that we are slightly abusing notation and denote variables, $\dot{\mathbf{q}}$, and function, $\dot{\mathbf{q}}(\mathbf{x}_\neq(t_0), \mathbf{x}_\partial, \mathbf{q})$, using the same symbols.

If some of the boundary neurons $\tilde{\mathbf{x}}_\partial$ take continuous values and others $\bar{\mathbf{x}}_\partial$ only discrete values, i.e.

$$p_{\bar{\mathbf{x}}_\partial}(\bar{\mathbf{x}}_\partial) = \sum_\alpha A_\alpha \delta^{(\tilde{N}_\partial)}(\bar{\mathbf{x}}_\partial - \mathbf{X}_\alpha), \quad (3.10)$$

then (3.9) can be integrated over $\bar{\mathbf{x}}_\partial$ to obtain

$$p_{\dot{\mathbf{q}}}(\dot{\mathbf{q}}|\mathbf{q}) = \sum_\alpha A_\alpha \int p_{\tilde{\mathbf{x}}_\partial}(\tilde{\mathbf{x}}_\partial|\mathbf{X}_\alpha) \delta^{(K)}(\dot{\mathbf{q}} - \dot{\mathbf{q}}(\mathbf{x}_\partial|\mathbf{x}_\neq(t_0), \mathbf{q})) d^{\tilde{N}_\partial} \tilde{x}_\partial, \quad (3.11)$$

where $\dim(\bar{\mathbf{x}}) = \tilde{N}_\partial$, $\dim(\tilde{\mathbf{x}}) = \tilde{N}_\partial$ and $\tilde{N}_\partial + \tilde{N}_\partial = N_\partial$. In this case, the distribution of jumps of the trainable variables takes the form of a sum of terms, but in the following sections we will consider only one term at a given time and so for brevity of notations we shall omit tildes and α 's,

$$p_{\dot{\mathbf{q}}}(\dot{\mathbf{q}}|\mathbf{q}) = \int p_{x_\partial}(\mathbf{x}_\partial) \delta^{(K)}(\dot{\mathbf{q}} - \dot{\mathbf{q}}(\mathbf{x}_\partial|\mathbf{x}_\neq(t_0), \mathbf{q})) d^{N_\partial} x_\partial. \quad (3.12)$$

If $K > N_\partial$, then we should be able to perform a local coordinate transformation

$$q'_i = \Lambda_i^j q_j. \quad (3.13)$$

so that $K - N_\partial$ direction become constrains, i.e. $\dot{q}'_i = 0$ for $i = N_\partial + 1, \dots, K$ and then the tangent vector $\dot{\mathbf{q}}$ can be projected onto N_∂ -dimensional dynamical subspace,

$$\dot{q}'^r = R_j^r \Lambda_i^j \dot{q}^i \quad (3.14)$$

where all of the components are dynamical. By integrating over $K - N_\partial$ constrained directions we obtain

$$p_{\dot{\mathbf{q}}}(\dot{\mathbf{q}}|\mathbf{q}) = \int p_{x_\partial}(\mathbf{x}_\partial) \delta^{(N_\partial)}(\dot{\mathbf{q}} - \dot{\mathbf{q}}(\mathbf{x}_\partial|\mathbf{x}_\partial(t_0), \mathbf{q})) d^{N_\partial} x_\partial. \quad (3.15)$$

If the map $\dot{\mathbf{q}}(\mathbf{x}_\partial|\mathbf{x}_\partial(t_0), \mathbf{q})$ is reversible, then it can be considered as a true duality and then the probability distributions are related through Jacobian matrix

$$p_{\dot{\mathbf{q}}}(\dot{\mathbf{q}}) = p_{x_\partial}(\mathbf{x}_\partial) \left| \det \left(\frac{\partial \dot{q}'^r}{\partial x_\partial^l} \right) \right|^{-1}. \quad (3.16)$$

We shall refer to this map as the dataset-learning duality. For non-invertible maps Eq. (3.16) must include summation over different \mathbf{x}_∂ that are mapped to the same $\dot{\mathbf{q}}$. However, even in this more general case, the contribution from a single term in the summation might dominate (e.g., if $p_{x_\partial}(\mathbf{x}_\partial)$ dominates for some \mathbf{x}_∂), and then Eq. (3.16) would still be approximately satisfied.

4 Jacobian matrix

For subsequent discussions, we need to obtain an expression for the Jacobian in Eq. (3.16). The gradient descent equation (3.7) in the transformed variables (3.14) becomes:

$$\begin{aligned} \ddot{q}'^r(\mathbf{x}_\partial|\mathbf{q}) &= -\gamma R_i^r \Lambda_j^i \Lambda_k^j \frac{\partial H(\mathbf{f}, \mathbf{x}_\partial, \mathbf{q})}{\partial q_k} \\ &= -\gamma R_i^r \Lambda_j^i \Lambda_k^j \left(\frac{\partial f_m}{\partial q_k} \frac{\partial H_x}{\partial f_m} + \frac{\partial H_q}{\partial q_k} \right). \end{aligned} \quad (4.1)$$

and then the Jacobian matrix can be expressed as

$$\frac{\partial \dot{q}'^r}{\partial x_\partial^l} = -\gamma (R\Lambda^2)^r_k \left(\frac{\partial^2 f_m}{\partial x_\partial^l \partial q_k} \frac{\partial}{\partial f_m} + \frac{\partial f_m}{\partial q_k} \frac{\partial^2}{\partial x_\partial^l \partial f_m} \right) H_x(\mathbf{f}, \mathbf{x}_\partial). \quad (4.2)$$

By substituting it back to (3.16) we obtain an expression for probability distribution of fluctuations of trainable variables

$$p_{\dot{\mathbf{q}}}(\dot{\mathbf{q}}) = \gamma^{-N} p_{x_\partial}(\mathbf{x}_\partial) \left| \det \left(R\Lambda^2 \left(\frac{\partial^2 f_m}{\partial x_\partial^l \partial q_r} \frac{\partial}{\partial f_m} + \frac{\partial f_m}{\partial q_r} \frac{\partial^2}{\partial x_\partial^l \partial f_m} \right) H_x(\mathbf{f}, \mathbf{x}_\partial) \right) \right|^{-1} \quad (4.3)$$

with three factors:

1. $p_{x_\partial}(\mathbf{x}_\partial)$ - distribution of non-trainable input neurons
2. $\frac{\partial H_x}{\partial f_m}; \frac{\partial^2 H_x}{\partial x_\partial^l \partial f_m}$ - Jacobian and Hessian of the loss function
3. $\frac{\partial^2 f_m}{\partial x_\partial^l \partial q_r}; \frac{\partial f_m}{\partial q_r}$ - tensors, which may be difficult to calculate directly, express the dependence of the result (e.g. prediction) \mathbf{f} obtained by the neural network on the boundary parameters \mathbf{x}_∂ and trainable variables \mathbf{q} .

The first factor depends directly on the boundary dynamics, i.e. training dataset, the second factor depends on the learning dynamics, i.e. the loss function, and the third factor depends on the activation dynamics, i.e. activation function.

To proceed further, we shall perform coordinate transformations so that the Jacobian becomes diagonal. This way, the local fluctuation of each trainable parameter would be influenced solely by the value of a single non-trainable variable, resulting in dimensional reduction. The Jacobian can be diagonalized locally using singular value decomposition,

$$J_j^i = \frac{\partial \hat{q}^i}{\partial x_\partial^j} = U_l^i \hat{\Sigma}_k^l V_j^{Tk}, \quad (4.4)$$

where $\hat{\Sigma}$ is a diagonal matrix, \hat{U} and \hat{V} are orthogonal matrices of left and right singular vectors. These matrices can be used to transform trainable and non-trainable variables

$$\begin{aligned} q'_i &= (U^T)_i^j q_j, \\ x_\partial^i &= (V^T)_j^i x_\partial^j \end{aligned} \quad (4.5)$$

and then the duality expression (3.16) can be rewritten in terms of the primed variables, but for brevity of notations and without losing the generality we drop primes.

Furthermore, we can omit the transformation matrices R and Λ assuming that we are already in the rotated variables and then the local N_∂ -dimensional duality (4.3) can be expressed as N_∂ decoupled equations,

$$p_{q^i}(\hat{q}^i) = p_{x_\partial^i}(x_\partial^i) \left| \frac{\partial \hat{q}^i}{\partial x_\partial^i} \right|^{-1}, \quad (4.6)$$

i.e. one for each dimension. Note that we need not make any assumptions about factorization of the probability distribution $p_{\hat{q}^i}$, since in the transformed coordinates all of learning directions are linearly independent. Therefore, by substituting expression for diagonalized Jacobian (4.2) into formula (4.6), we can obtain a set of equations for the distributions of fluctuations of linearly independent trainable variables q_i 's.

5 Toy model

In the previous section, we discussed how a general multidimensional problem can be reduced to a set of decoupled (or perhaps weakly coupled) one-dimensional ones (4.6). In this section, we shall consider a concrete example of a simple two-dimensional problem.

Consider a neural network consisting of only two neurons: input x_1 and output x_2 connected by a trainable weight $w = w_{21}$ and a bias $b = b_2$. In addition, we assume that the output neuron can take only two possible values, i.e. its marginal distribution is a sum of two delta functions as in Eq. (3.10),

$$p_{x_2}(x_2) = \frac{1}{2}\delta(x_2 - X_1) + \frac{1}{2}\delta(x_2 - X_2). \quad (5.1)$$

In this case, we can reduce the two-dimensional problem (i.e. two trainable variables w and b and two non-trainable variables x_1 and x_2) to two one-dimensional ones, corresponding to two different values, $x_2 = X_1$ and $x_2 = X_2$ as in Eq. (3.11).

To accomplish this task we must determine the direction along which trainable variables change $\dot{\mathbf{q}} = (\dot{w}, \dot{b})$ due to changes in the state of input neuron x_1 . Note that we will consider the values of the trainable variables to be approximately constant and consider fluctuations around its equilibrium value. For this simple problem we can define two non-local transformations $\mathbf{q} \rightarrow \mathbf{q}_1$ and $\mathbf{q} \rightarrow \mathbf{q}_2$ for respectively $x_2 = X_1$ and $x_2 = X_2$ such that

$$\begin{aligned} \dot{\mathbf{q}}'_1 &= \left(\sqrt{\dot{w}^2(x_1, X_1) + \dot{b}^2(x_1, X_1)}, 0 \right) \\ \dot{\mathbf{q}}'_2 &= \left(\sqrt{\dot{w}^2(x_1, X_2) + \dot{b}^2(x_1, X_2)}, 0 \right) \end{aligned} \quad (5.2)$$

In what follows, to simplify the notation, the primes will be discarded as usual, and \dot{q} will be understood as its first component, i.e.

$$\begin{aligned} \dot{q}_1(x_1) &= \sqrt{\dot{w}^2(x_1, X_1) + \dot{b}^2(x_1, X_1)} \\ \dot{q}_2(x_1) &= \sqrt{\dot{w}^2(x_1, X_2) + \dot{b}^2(x_1, X_2)}. \end{aligned} \quad (5.3)$$

For the resulting one-dimensional problems, we can use the dataset-learning duality mapping (4.6) to express distribution of fluctuations of the only remaining trainable variable \dot{q}_1 (or \dot{q}_2) in terms of the distribution of the input neuron x_1 , i.e.

$$\begin{aligned} p_{\dot{q}}(\dot{q}) &= p_{x_1}(x_1) \left| \frac{d\dot{q}}{dx_1} \right|^{-1} \\ &= p_{x_1}(x_1) \left| \frac{\dot{w}}{\dot{q}} \frac{d\dot{w}}{dx_1} + \frac{\dot{b}}{\dot{q}} \frac{d\dot{b}}{dx_1} \right|^{-1} \\ &= p_{x_1}(x_1) \left| \cos \alpha \frac{d\dot{w}}{dx_1} + \sin \alpha \frac{d\dot{b}}{dx_1} \right|^{-1}, \end{aligned} \quad (5.4)$$

where α is the rotation angle in transformations (5.2). Note that $\tan \alpha$ determines relative contributions from fluctuations of weights and bias fluctuations in the full Jacobian and, as a consequence, in the distribution of \dot{q} .

6 Emergent criticality

In this section, we shall utilize the dataset-learning duality (see Sec. 3) to investigate the potential emergence of criticality arising mainly from the Jacobian matrix (see Sec. 4) within the context of the toy model (see Sec. 5). The idea is to determine conditions under which the criticality might emerge in the toy model and then verify the results numerically for a toy-model classification problem. Specifically, our aim is to identify compositions of activation and loss functions that give us a power-law dependence of the Jacobian leading to a power-law distribution of fluctuations in the trainable variables.

For the toy model introduced in the previous section, the power-law dependence of the Jacobian (for changes of weights with respect to the state of input neuron) is given by

$$\frac{d\dot{w}}{dx_1} = (A\dot{w} + B)^{k_w}, k_w > 0. \quad (6.1)$$

and a similar expression can be obtained for changes in biases. Note that we expect that $k_w > 0$ (which corresponds to a power-law suppression of larger fluctuations) and coefficients $A = A(w, b); B = B(w, b)$ are function of the equilibrium weight w and bias b , but not on the input state x_1 . According to the stochastic gradient descent method (2.3) with mini-batch size $M = 1$,

$$\dot{w} = -\gamma \frac{\partial H}{\partial w}. \quad (6.2)$$

Together Eqs. (6.1) and (6.2) is a system of differential equations that must be solved in order to determine suitable compositions of activation and loss functions.

The first equation (6.1) has two solutions

$$\dot{w} = \begin{cases} \exp(Ax_1 + B) & \text{for } k_w = 1 \\ (Ax_1 + B)^{\frac{1}{1-k_w}} & \text{for } k_w \neq 1 \end{cases} \quad (6.3)$$

for some other constants $A = A(w, b); B = B(w, b)$ and, under assumption that the composition of loss and activation functions is a function of $y \equiv wx_1 + b$, the second equation (6.2) becomes

$$\dot{w} = -\gamma x_1 \frac{\partial H}{\partial y}. \quad (6.4)$$

For $k_w = 1$ we obtain a differential equations for loss function which admits power-law fluctuations,

$$(y - b) \frac{\partial H}{\partial y} = \exp(Ay + B) + C \quad (6.5)$$

whose solution is given by

$$H(y) = \exp(Ab + B) Ei(A(y - b)) + C \log(y - b) \quad (6.6)$$

where $Ei(x) = -\int_{-x}^{\infty} t^{-1}e^{-t}dt$ is the exponential integral. For $C \sim 0$ and $|y-b| \gg A^{-1}$ we get

$$H(y) \approx \frac{\exp(Ay + B)}{A(y-b)} = \exp(Ay + B - \log A(y-b)) \approx \exp(Ay + B) \quad (6.7)$$

or

$$\boxed{H(y) \approx \exp(c_1y + c_2)}. \quad (6.8)$$

where c_1 and c_2 are numerical constants, and the following condition must be satisfied,

$$|wx_1| \gg c_1^{-1}. \quad (6.9)$$

7 Power-law map

In this section we study the second case in Eq. (6.3), i.e. $k_w \neq 1$, which describes a power-law duality map from the non-trainable variable x_1 to the tangent space of the trainable variable,

$$\dot{w}(x_1) = (Ax_1 + B)^{\frac{1}{1-k_w}}. \quad (7.1)$$

The goal is to determine all of the allowed values for k_w where A and B are function of weight and bias, i.e. $A(w, b)$ and $B(w, b)$. By substituting Eq. (7.1) into Eq. (6.4) we obtain a differential equations for loss function which admits power-law fluctuations of the trainable weight,

$$(y-b) \frac{\partial H}{\partial y} = (Ay + B)^{\frac{1}{1-k_w}} + C, \quad (7.2)$$

where $A(w, b)$ and $B(w, b)$ are some other functions. Our assumption is that the composition of loss and activation function $H(y)$ (separately for each class in our toy-model) depends only on the argument $y = wx + b$ of the activation function. Thus, it is sufficient to consider possible compositions of activation and loss functions, rather than each separately. There are only three cases to consider:

- Case $k_w = 0$. By integrating (7.2) we get that

$$H(y) = (Ab + B + C) \log(y-b) + Ay + \text{const} \quad (7.3)$$

which does not depend on b only if

$$\begin{cases} A = \text{const} \\ Ab + B + C = 0, \end{cases} \quad (7.4)$$

or a linear function

$$\boxed{H(y) = c_1y + c_2} \quad (7.5)$$

for some numerical constants c_1 and c_2 .

- Case $k_w = 1/2$. By integrating (7.2) we get that

$$H(y) = (A^2b^2 + 2AbB + B^2 + C) \log(y - b) + Ay(2B + A(b + y/2)) + \text{const} \quad (7.6)$$

which does not depend on b only if

$$\begin{cases} A = \text{const}, \\ A^2b^2 + 2AbB + B^2 + C = 0, \\ 2B + Ab = \text{const}, \end{cases} \quad (7.7)$$

or a quadratic function

$$\boxed{H(y) = c_1y^2 + c_2y + c_3} \quad (7.8)$$

for some numerical constants c_1 , c_2 and c_3 .

- Case $k_w \neq 0$ and $k_w \neq 1/2$. For more general k_w it is useful to take the first derivative of (7.2) with respect to w and the second derivative with respect to b :

$$\begin{cases} \frac{1}{1-k_w}(Ay + B)^{\frac{k_w}{1-k_w}}(A_wy + B_w) + C_w = 0, \\ \frac{1}{1-k_w}(Ay + B)^{\frac{2k_w-1}{1-k_w}} \left[\left(\frac{k_w}{1-k_w} \right) (A_by + B_b)^2 + (Ay + B)(A_{bb}y + B_{bb}) \right] + C_{bb} = 0. \end{cases}$$

Since these equations must be satisfied for any y , we obtain the following conditions

$$\begin{cases} A_w = B_w = C_w = C_{bb} = 0, \\ \frac{k_w}{1-k_w} A_b^2 (y + B_b/A_b)^2 + AA_{bb} (y + B/A) (y + B_{bb}/A_{bb}) = 0. \end{cases} \quad (7.9)$$

The second equation of (7.9) can be represented as a system

$$\begin{cases} \frac{B}{A} = \frac{B_b}{A_b} = \frac{B_{bb}}{A_{bb}}, \\ \frac{k_w}{1-k_w} A_b^2 + AA_{bb} = 0. \end{cases} \quad (7.10)$$

whose solution is given by

$$A(b) = \frac{B(b)}{a} = c_2 \left(\frac{1}{1-k_w} b + c_1 \right)^{1-k_w}, \quad (7.11)$$

where we have also used that $A_w = B_w = 0$. Now, substituting (7.11) into (7.2) and setting $b = y$ we get

$$C = -c_2^{1-k_w} \left(\frac{1}{1-k_w} b + c_1 \right) (b + a)^{\frac{1}{1-k_w}}, \quad (7.12)$$

which can satisfy condition $C_w = 0$ and $C_{bb} = 0$, only if $k_w = 2$ and $c_1 = -a$, then $C = \frac{1}{c_2}$ and $A = -\frac{c_2}{b+a}$.

Integrating (7.2) for identified types of C , $A(b)$, $B(b)$, we get a logarithmic function

$$\boxed{H(y) = c_1 \log(c_2 + c_3y) + c_4} \quad (7.13)$$

for some numerical constants c_1 , c_2 , c_3 and c_4 .

Note, however, that the conditions (7.9) are necessary but not sufficient to obtain the power-law dependence $\dot{w}(x)$ (7.1). In fact it is easy to check that (7.13) is not a solution of (7.2).

We conclude that $k_w = 0$, $k_w = 1/2$ and $k_w = 1$ correspond to respectively linear (7.5), quadratic (7.8) and exponential (6.8) solutions for $H(y)$. By carrying out similar calculations for \dot{b} one can also show that $k_b = 0$, $k_b = 1$ and $k_b = 2$ correspond to respectively quadratic (7.8), exponential (6.8) and logarithmic (7.13) solutions for $H(y)$.

8 Numerical results

In this section, we shall present numerical results for the toy model described in Sec. 5, and compare them with analytical results obtained in Sec. 6 and 7. In particular, we are interested in studying the emergence of critical behavior, or when the distribution of changes in trainable variable q is described by a power-law, i.e.,

$$p(\dot{q}) \propto \dot{q}^{-k_q}. \quad (8.1)$$

The goal is to provide specific numerical examples of the critical behavior (8.1) on some ranges of scales for either quadratic (7.8), exponential (6.8) or logarithmic (7.13) compositions of activation and loss functions, i.e. for $H(y)$.

For the numerical experiments we consider a simple dataset with only two classes (called ‘zeros’ and ‘ones’) and so there is only a single output neuron which takes discrete values ($x_2 = 0$ or $x_2 = 1$). The input subspace also consists of only a single neuron that takes continuous values drawn from two Gaussian probability distribution $p_0(x_1)$ (for $x_2 = 0$) and $p_1(x_1)$ (for $x_2 = 1$) with mean

$$\begin{aligned} \langle x_1 \rangle_0 &= 0 \\ \langle x_1 \rangle_1 &= 1 \end{aligned} \quad (8.2)$$

and standard deviations

$$\begin{aligned} \sqrt{\langle x_1^2 \rangle_0 - \langle x_1 \rangle_0^2} &= \sqrt{\langle x_1^2 \rangle_0} = 0.25 \\ \sqrt{\langle x_1^2 \rangle_1 - \langle x_1 \rangle_1^2} &= \sqrt{\langle x_1^2 \rangle_1 - 1} = 0.25. \end{aligned} \quad (8.3)$$

This simple dataset allows us to use the architecture of the toy model of Sec. 5 with one input neuron x_1 , one output neuron x_2 , one trainable bias b and one trainable weight w (from input neuron to output neuron).

Note that the main goal of this analysis is not to obtain high prediction accuracy (although it is above 97% in all experiments), or to develop an architecture for a realistic classification problem (although a similar dataset would have been obtained if we considered a truncated MNIST dataset [18] with only images of ‘zeros’

and ‘ones’ and input states projected down to a single dimension). Rather, our aim is to demonstrate the emergence of criticality within a simple low-dimensional problem, but we expect the same mechanisms to be responsible for the emergence of criticality in higher-dimensional problems [16]. This is because, in the learning equilibrium, the high-dimensional problems can be linearized and reduced to many weakly coupled low-dimensional ones, as argued in Secs. 3 and 4.

Also, note that in the learning equilibrium, the average value of the trainable parameters does not change significantly. Therefore, the distribution of the actual changes of trainable variables, i.e., $p(\dot{q})$, and the distribution of potential jumps when the trainable parameters remain fixed, i.e., $p\left(-\gamma\frac{\partial H}{\partial q}\right)$, are essentially the same. However, the latter is more suitable if we are to consider potential jumps caused separately by ‘zeros’ and ‘ones’ classes, which, in the learning equilibrium, can be described by two one-dimensional problems.

In the remainder of the section we shall consider four experiments, two for exponential (6.8), one for quadratic (7.8), and one for logarithmic (7.13) composition of activation and loss functions.

8.1 Exponential composition, $k_q = 1$

Consider sigmoid activation function

$$f = (1 + e^{-y})^{-1} \quad (8.4)$$

with mean squared loss

$$H(f) = (f - x_2)^2 \quad (8.5)$$

or cross-entropy loss function

$$H(f) = -(1 - x_2) \log(1 - f) - x_2 \log(f). \quad (8.6)$$

For composition of sigmoid activation (8.4) and mean squared loss (8.5) functions and ‘zeros’ class, in the limit

$$wx_1 \ll -b \quad (8.7)$$

Eq. (8.4) reduces to

$$f \approx e^y, \quad (8.8)$$

and then

$$H(f) = f^2 \approx e^{2y}, \quad (8.9)$$

which is the exponential in Eq. (6.8) with $c_1 = 2, c_2 = 0$. For the exponential composition changes of weight and bias are given by

$$\dot{b} = -2\gamma \exp(wx_1 + b) \quad (8.10)$$

$$\dot{w} = x_1 \dot{b} \quad (8.11)$$

and fluctuations in the relevant trainable direction are described by $k_q = 1$, i.e.

$$p_{\dot{q}}(\dot{q}) = p_{x_1}(x_1) \left| \frac{d\dot{q}}{dx_1} \right|^{-1} \propto \dot{q}^{-1}, \quad (8.12)$$

since the Jacobian is given by

$$\left| \frac{d\dot{q}}{dx_1} \right| = \left| \frac{\dot{w}}{\dot{q}} \frac{d\dot{w}}{dx_1} + \frac{\dot{b}}{\dot{q}} \frac{d\dot{b}}{dx_1} \right| = \frac{2|w|\dot{w}^2 + \dot{b}\dot{w} + 2|w|\dot{b}^2}{\dot{q}} \approx 2|w| \frac{\dot{w}^2 + \dot{b}^2}{\dot{q}} \propto \dot{q} \quad (8.13)$$

where we used Eqs. (5.3) and (5.4) and assumed

$$|w| \gg 1. \quad (8.14)$$

Then the range of x_1 for which the Jacobian is a power-law is described by conditions (6.9), (8.14) and (8.7), or

$$\frac{1}{2} \ll |wx_1|, \quad |w| \gg 1 \quad \text{and} \quad wx_1 \ll -b. \quad (8.15)$$

These conditions are used to obtain a range for x_1 where the power-law distribution is expected which then gives us a range for \dot{q} (5.3). On Fig. 1 distribution of negative fluctuations $\log(p_{\dot{q}}(\dot{q}))$ is plotted with dotted blue line, contribution from Jacobian $\log\left(\frac{\partial x_1}{\partial \dot{q}}\right)$ with red line and conditions where the power-law is expected with vertical dashed green bars. Note that the plot is $\log(p_{\dot{q}}(\dot{q}))$ vs. $\log(\dot{q})$ and all power-law functions, e.g. $p_{\dot{q}}(\dot{q}) = A\dot{q}^{-k_q}$, must appear as straight lines with slopes equal to the power, i.e. $\log(p_{\dot{q}}(\dot{q})) = \log(A) - k_q \log(\dot{q})$. The same log-log plots, with the same colors and styles, will be used in all subsequent figures.

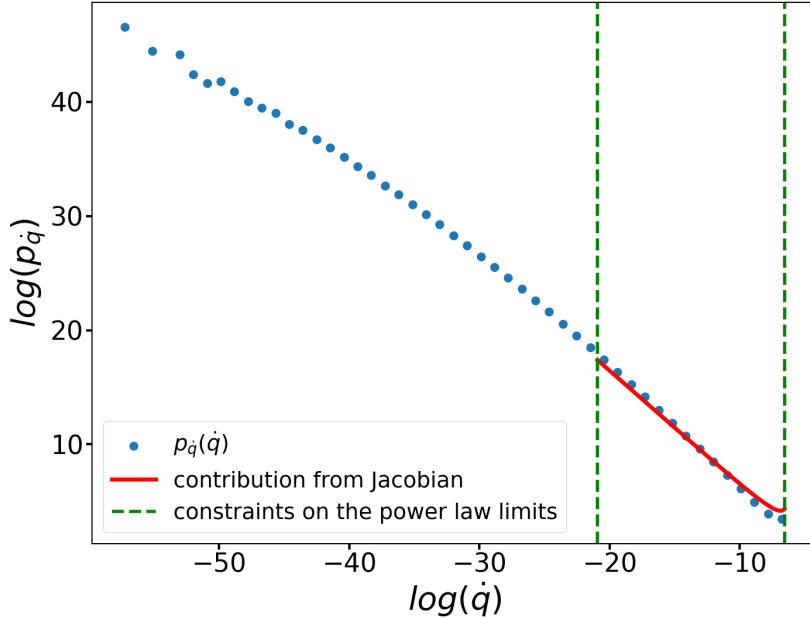


Figure 1. Distribution of negative fluctuations for 'zeros' class for composition of sigmoid activation and mean squared loss functions.

For composition of sigmoid activation (8.4) and mean squared loss (8.5) functions and ‘ones’ class, in the limit

$$wx_1 \gg -b, \quad (8.16)$$

Eq. (8.4) reduces to

$$f \approx 1 - e^{-y}. \quad (8.17)$$

and then

$$H = (1 - f)^2 \approx e^{-2y}. \quad (8.18)$$

which is the exponential Eq.(6.8) with $c_1 = -2, c_2 = 0$.

The range of x_1 for which the Jacobian is a power-law is described by conditions (6.9), (8.14) and (8.16), or

$$\frac{1}{2} \ll |wx_1|, \quad |w| \gg 1 \quad \text{and} \quad wx_1 \gg -b. \quad (8.19)$$

On Fig. 2 distribution of positive fluctuations $\log(p_{\dot{q}})$ is plotted.

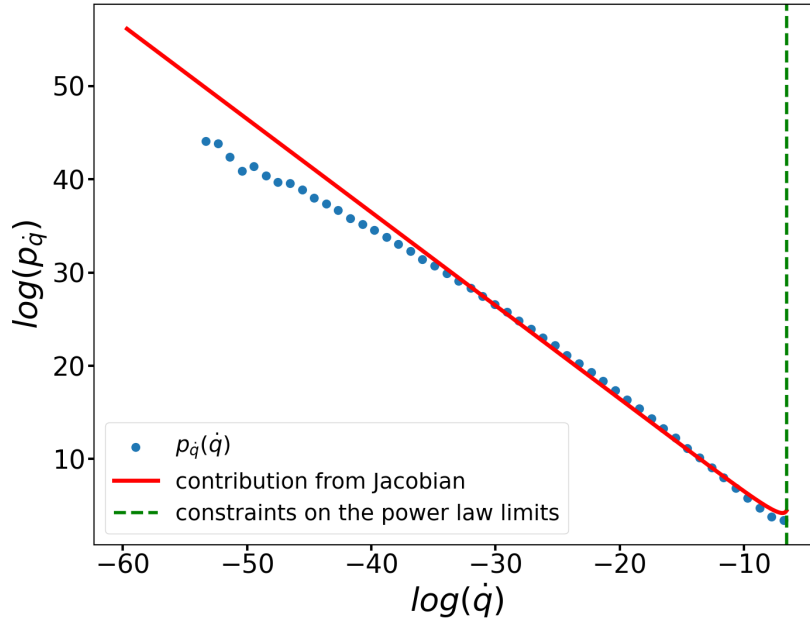


Figure 2. Distributions of positive fluctuations for ‘ones’ class for composition of sigmoid activation and mean squared loss functions.

By following the same analysis for composition of sigmoid activation (8.4) and cross-entropy loss (8.6) function we obtain, for ‘zeros’ class:

$$H = -\log(1 - f) \approx e^y \quad (8.20)$$

and

$$1 \ll |wx_1|, |w| \gg 1 \quad \text{and} \quad wx_1 \ll -b \quad (8.21)$$

and for ‘ones’ class:

$$H = \log(f) \approx e^{-y} \quad (8.22)$$

and

$$1 \gg |wx_1|, |w| \gg 1 \quad \text{and} \quad wx_1 \gg -b. \quad (8.23)$$

On Figs. 3 and 4 distributions of negative fluctuations for ‘zeros’ class and positive fluctuations for ‘ones’ class $\log(p_{\dot{q}}(\dot{q}))$ are plotted, respectively. Note that although the power-law contribution from Jacobian is expected on a wide ranged of scales, i.e. between vertical dashed green bars, in this example a significant contribution comes from the dataset, i.e. $p_1(x_1)$ or $p_1(x_1)$, which is Gaussian.

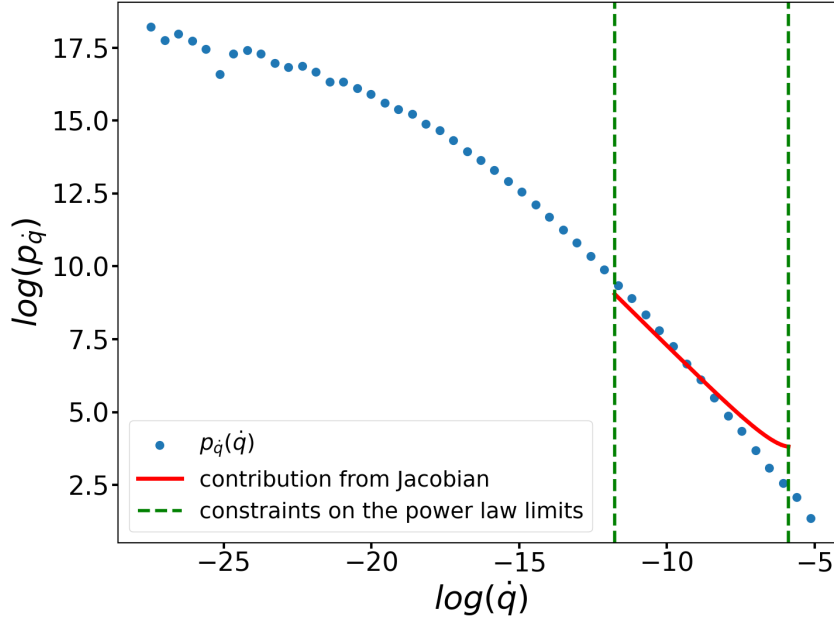


Figure 3. Distributions of negative fluctuations for ‘zeros’ class for composition of sigmoid activation and cross-entropies.

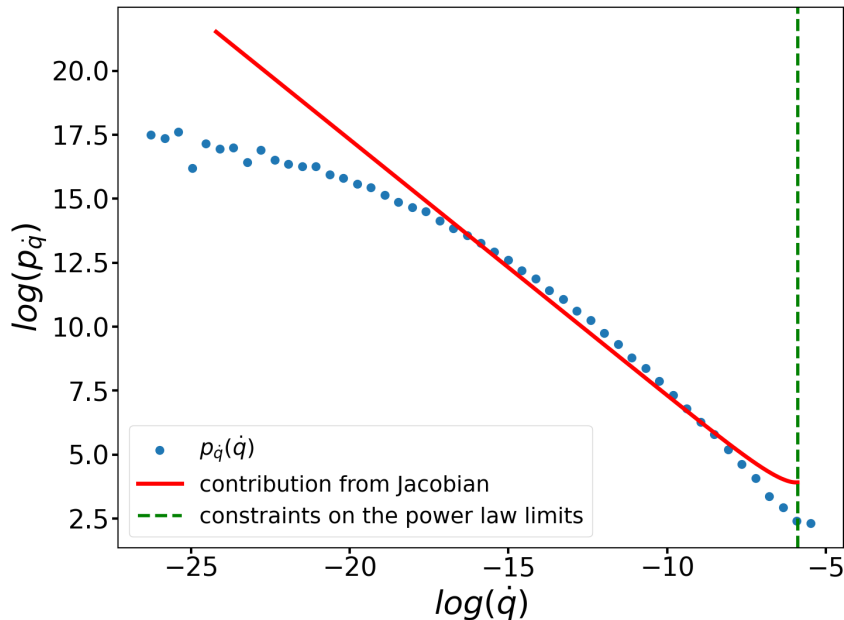


Figure 4. Distributions of positive fluctuations for 'ones' class for composition of sigmoid activation and cross-entropy loss functions.

We conclude that for the toy-model classification problem with a sigmoid activation function and either mean squared error or cross-entropy loss functions, the fluctuations of trainable variables can follow a power law with $k_q = -1$, as confirmed both numerically and analytically.

8.2 Quadratic composition, $k_q = 0$

Consider a composition of a ReLU activation function

$$f(y) = \max(0, y) \tag{8.24}$$

and mean squared loss function

$$H(f) = (f - x_2)^2. \tag{8.25}$$

In this case, non-vanishing fluctuations can take place only when the argument of ReLU is positive, i.e.

$$wx_1 > -b, \tag{8.26}$$

or when the composition function is quadratic (7.8)

$$H(y) = (y - x_2)^2. \tag{8.27}$$

For the quadratic composition, changes of weight and bias are given by

$$\dot{b} = -\gamma \frac{\partial H}{\partial b} = -2\gamma(wx_1 + b - x_2) \quad (8.28)$$

$$\dot{w} = x_1 \dot{b} \quad (8.29)$$

and fluctuations in the relevant trainable variables are described by $k_q = 0$, i.e.

$$p_{\dot{q}}(\dot{q}) = p_{x_1}(x_1) \left| \frac{d\dot{q}}{dx_1} \right|^{-1} \propto \text{const}, \quad (8.30)$$

since the Jacobian is given by

$$\frac{d\dot{q}}{dx_1} = \left| \frac{\dot{w}}{\dot{q}} \frac{d\dot{w}}{dx_1} + \frac{\dot{b}}{\dot{q}} \frac{d\dot{b}}{dx_1} \right| = \frac{1}{\dot{q}} |x_1 \dot{b}^2 - 2\gamma w x_1^2 \dot{b}^2 - 2\gamma w \dot{b}| \approx \frac{1}{\dot{q}} |2\gamma w \dot{b}| \approx |2\gamma w| \quad (8.31)$$

where

$$x_1 \ll 1 \quad \text{and} \quad (|x_1 \dot{b}| \ll 2\gamma |w| \quad \text{or} \quad |x_1(w x_1 + b - x_2)| \ll |w|). \quad (8.32)$$

On Fig. 5 distribution of negative fluctuations for ‘zeros’ class $\log(p_{\dot{q}}(\dot{q}))$ is plotted. The deviation of the Jacobian from a constant is due to non-linearity of the dependence $x_1(\dot{q})$, when $x_1 \sim 1$.

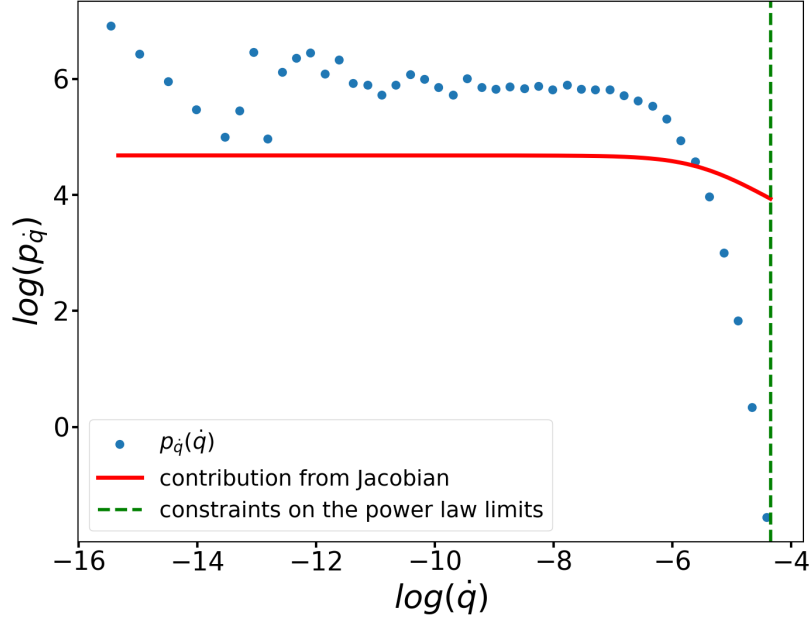


Figure 5. Distributions of negative fluctuations for ‘zeros’ class for composition of ReLU activation and mean squared loss.

8.3 Logarithmic composition, $k_q = -2$

Consider the cross-entropy loss function (8.6) and a piece-wise linear activation function

$$f(y) = \begin{cases} y, & 0 < |wx_1 + b| < 1, \\ 0, & |wx_1 + b| < 0 \text{ or } |wx_1 + b| > 1. \end{cases} \quad (8.33)$$

In this case, power-law fluctuations can take place in the range between $-\frac{b}{w}$ and $\frac{1-b}{w}$, i.e.

$$-\frac{b}{w} < x_1 < \frac{1-b}{w} \quad \text{or} \quad \frac{1-b}{w} < x_1 < -\frac{b}{w}. \quad (8.34)$$

Within this range, the composition function is

$$H(y) = -(1-x_2) \log(1-y) - x_2 \log(y). \quad (8.35)$$

which is the logarithm composition of (7.13) for 'zeros' class (i.e. $x_2 = 0$) with

$$c_1 = -1, c_2 = 1, c_3 = -1 \quad \text{and} \quad c_4 = 0, \quad (8.36)$$

and for 'ones' class (i.e. $x_2 = 1$) with

$$c_1 = -1, c_2 = 0, c_3 = 1 \quad \text{and} \quad c_4 = 0. \quad (8.37)$$

For the 'zeros' class and logarithmic composition (7.13), changes of weight and bias are given by

$$\dot{b} = -\gamma \frac{\partial H}{\partial b} = -\gamma \frac{1}{1-wx_1-b} \quad (8.38)$$

$$\dot{w} = x_1 \dot{b} \quad (8.39)$$

and fluctuations in the relevant trainable variables are described by $k_q = 2$, i.e.

$$p_{\dot{q}}(\dot{q}) = p_{x_1}(x_1) \left| \frac{d\dot{q}}{dx_1} \right|^{-1} \propto \dot{q}^{-2}, \quad (8.40)$$

since the Jacobian is given by

$$\begin{aligned} \left| \frac{d\dot{q}}{dx_1} \right| &= \left| \frac{\dot{w}}{\dot{q}} \frac{d\dot{w}}{dx_1} + \frac{\dot{b}}{\dot{q}} \frac{d\dot{b}}{dx_1} \right| = \left| \frac{\dot{w}}{\dot{q}} \left(\dot{b} - \frac{\gamma x_1 w}{(1-wx_1-b)^2} \right) - \frac{\dot{b}}{\dot{q}} \frac{\gamma w}{(1-wx_1-b)^2} \right| = \\ &= \frac{1}{\dot{q}} \left| x_1 \dot{b}^2 - \frac{wx_1^2 \dot{b}^2}{1-wx_1-b} - \frac{w\dot{b}^2}{1-wx_1-b} \right| \approx \frac{1}{\dot{q}} \frac{|w|\dot{b}^2}{1-wx_1-b} \approx \frac{|w\dot{b}|}{1-wx_1-b} \approx \frac{|w|\dot{q}^2}{\gamma}, \end{aligned} \quad (8.41)$$

where

$$x_1 \ll 1 \quad \text{and} \quad (1-wx_1-b)|x_1| \ll |w|. \quad (8.42)$$

Similar reasoning can be carried out for the 'ones' class.

On Figs. 6 and 7 distributions of negative fluctuations for ‘zeros’ class and positive fluctuations for ‘ones’ class $\log(p_{\dot{q}})$ are plotted, respectively.

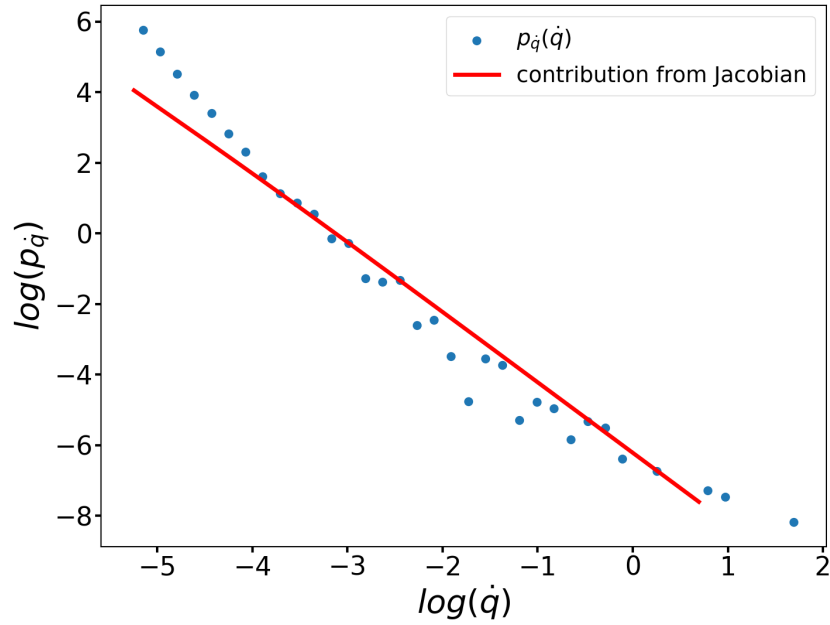


Figure 6. Distributions of negative fluctuations for ‘zeros’ class for composition of a piecewise linear activation and cross-entropy loss functions.

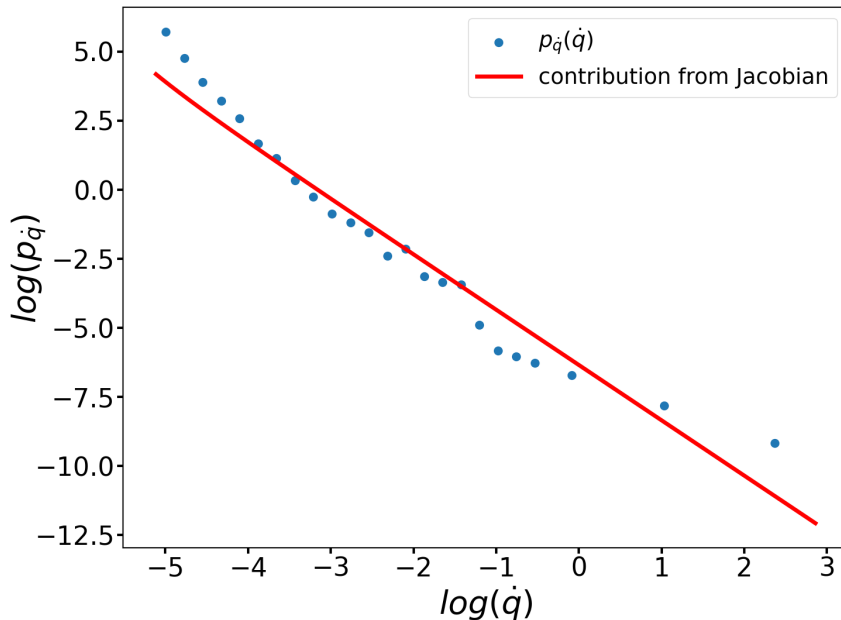


Figure 7. Distributions of negative fluctuations for ‘ones’ class for composition of a piecewise linear activation and cross-entropy loss functions.

9 Fractional powers

In Sec. 7 we argued that for a power law map (7.1), the power-law distribution, i.e.

$$p(\dot{w}) \propto \dot{w}^{-k_w}, \quad (9.1)$$

exists only for $k_w = 0, 1/2$ and 2 . However, if we are interested in approximate criticality, then we can just expand $\dot{w}(x_1)$ around $x_1 = \bar{x}$ and assume that only a single term dominates, i.e

$$\dot{w} = -\gamma \frac{\partial H}{\partial w} = -\gamma x_1 \frac{\partial H}{\partial y} = \sum_n \frac{1}{n!} A_n (x_1 - \bar{x})^n \approx \frac{A_m}{m!} (x_1 - \bar{x})^m. \quad (9.2)$$

In this case, the Jacobian is given by

$$\frac{d\dot{w}}{dx_1} = \frac{m\dot{w}}{(x_1 - \bar{x})} = \left(\frac{A_m}{m!} \right)^{\frac{1}{m}} m\dot{w}^{\frac{m-1}{m}}, \quad (9.3)$$

which allows fluctuations (4.6) to be given by more general (or fractional) powers,

$$p(\dot{w}) \propto \dot{w}^{-\frac{m-1}{m}}. \quad (9.4)$$

or

$$k_w = \frac{m-1}{m} \quad (9.5)$$

for $m \in \mathbb{N}$.

Consider the following composition function

$$\boxed{H(y) = c_2(y + c_1)^n}, \quad (9.6)$$

whose derivative is

$$h(y) = \frac{\partial H}{\partial y} = nc_2(y + c_1)^{n-1}, \quad (9.7)$$

and

$$\dot{w} \propto nc_2(y + c_1)^{n-1} \frac{y-b}{w} = \frac{nc_2}{w}(y + c_1)^n - \frac{nc_2(b + c_1)}{w}(y + c_1)^{n-1}. \quad (9.8)$$

where c_1 and c_2 are arbitrary numeric constants. For only a single term to dominate (as in Eq. (9.2)) we must set $\bar{x} = -\frac{c_1+b}{w}$ and then

$$\dot{w} \approx nc_2 w^{n-1} (x_1 - \bar{x})^n, \quad \text{when } |x_1| \gg \left| \frac{b + c_1}{w} \right| \quad (9.9)$$

or

$$\dot{w} \approx -nc_2(b + c_1)w^{n-2}(x_1 - \bar{x})^{n-1}, \quad \text{when } |x_1| \ll \left| \frac{b + c_1}{w} \right|. \quad (9.10)$$

Let's come back to the toy model classification problem from the previous section with two classes of 'zeros' and 'ones' (i.e. $x_2 = 0$ and $x_2 = 1$). For this simple learning task we can consider a power-law loss function

$$H(f) \propto (f - x_2)^{2m} \quad \text{for } m \in \mathbb{N}. \quad (9.11)$$

which can be considered as a generalization of the mean squared loss (8.25). Then if we set $c_1 = -x_2$ and $n = 2m$, then the composition of loss (9.11) and piece-wise linear activation takes the desired form of Eq. (9.6) in a region where the activation function is linear. For example, for ReLU (8.24) the region is given by

$$wx_1 + b > 0. \quad (9.12)$$

In addition, one of the conditions (9.9) or (9.10) must be satisfied, i.e.

$$|x_1| \gg \left| \frac{b - x_2}{w} \right|. \quad (9.13)$$

or

$$|x_1| \ll \left| \frac{b - x_2}{w} \right| \quad (9.14)$$

Next we consider a special case $n = 4$ (or $m = 2$) and apply Eqs. (5.3) and (5.4) to two conditions (9.13) and (9.14) separately.

- If (9.13) is satisfied then we obtain

$$\begin{aligned} \dot{w} &\approx -\frac{4\gamma}{w}(y+x_2)^4, \quad \dot{b} = -4\gamma(y+x_2)^3 = \frac{\dot{w}}{w(y+x_2)} \Rightarrow \\ \dot{q} &\propto \dot{w} \sqrt{1 + \frac{1}{(w(wx_1 + b + x_2))^2}} \approx \dot{w} \Rightarrow \\ \left| \frac{dx_1}{d\dot{q}} \right| &\propto \dot{q}^{-\frac{3}{4}}. \end{aligned} \quad (9.15)$$

where in the second line an additional conditions was used:

$$\left| x_1 + \frac{b+x_2}{w} \right| \gg \frac{1}{w^2}. \quad (9.16)$$

- If (9.14) is satisfied then we obtain

$$\begin{aligned} \dot{w} &\propto \dot{b} \propto (y+x_2)^3 \Rightarrow \\ \dot{q} &\propto (wx_1 + b + x_2)^3 \Rightarrow \\ \left| \frac{dx_1}{d\dot{q}} \right| &\propto \dot{q}^{-\frac{2}{3}}. \end{aligned} \quad (9.17)$$

On Figs. 8 and 9 distributions of negative fluctuations for ‘zeros’ class and positive fluctuations for ‘ones’ class $\log(p_{\dot{q}}(\dot{q}))$ are plotted, respectively.

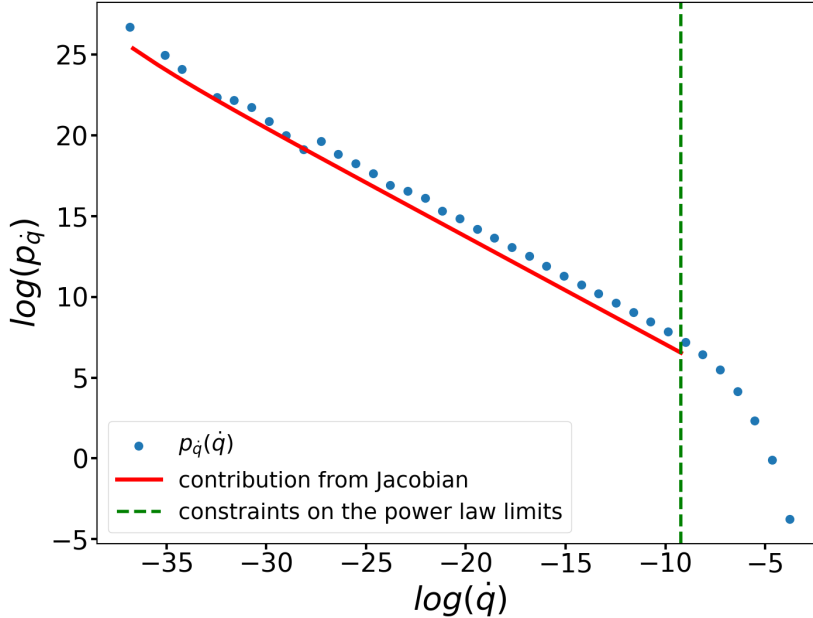


Figure 8. Distributions of negative fluctuations for ‘zeros’ class for composition of ReLU activation and quartic loss functions.

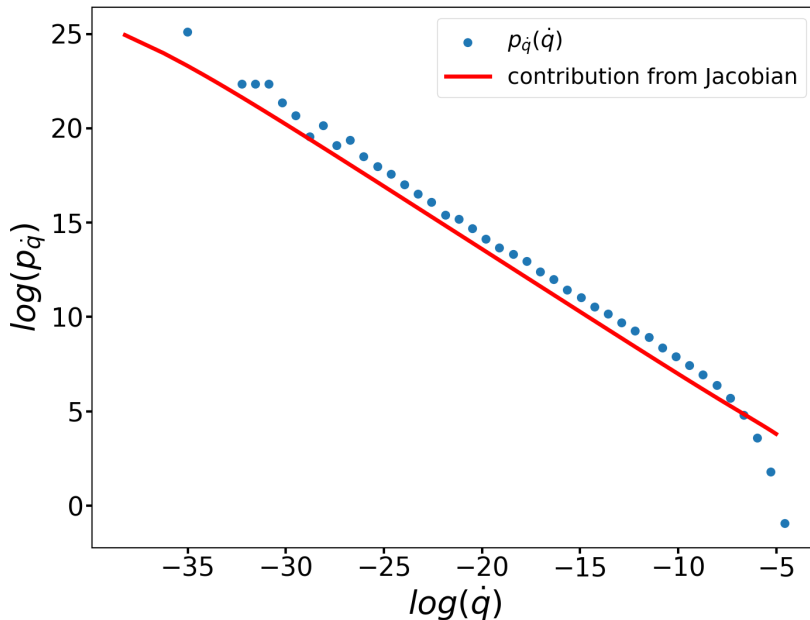


Figure 9. Distributions of positive fluctuations for ‘ones’ class. Combination of a fourth power loss function and a ReLU activation function.

10 Discussion

In this paper, we accomplished two main tasks.

Firstly, we established a duality mapping between the space of boundary neurons (i.e., the dataset) and the tangent space of trainable variables (i.e., the learning), the so-called dataset-learning duality. Both spaces (the boundary and the tangent) are generally very high-dimensional, making the analysis of the duality very non-trivial. However, in a local learning equilibrium, the calculations can often be simplified by replacing the multi-dimensional non-linear problem with many one-dimensional problems. If the interactions between the one-dimensional problems are weak, each of them can be analyzed separately with interactions considered perturbatively if necessary. Of course, the decoupling limit is not a generic limit, but it is within this limit that we were able to perform analytic calculations, which were then checked against numerical results.

Secondly, we applied the dataset-learning duality to study the emergence of criticality in the learning systems. In particular, by considering decoupled one-dimensional problems we analyzed different compositions of activation and loss function which can give rise to a power-law distribution of fluctuations of trainable variables on a wide range of scales. We showed that the power-law, exponential and logarithmic compositions of activation and loss can all give rise to criticality in the learning dynamics

even if the dataset is in a non-critical state. Main results of the study of criticality are summarized the following table, where c_1 , c_2 , c_3 and c_4 are arbitrary numeric constants.

k_w	k_b	$H(y)$	Examples
-	2	$c_1 \log(c_2 + c_3 y) + c_4$	Cross-entropy loss and piece-wise linear activation functions
$\frac{1}{2}$	0	$c_1 y^2 + c_2 y + c_3$	Mean squared loss and ReLU activation functions
1	1	$\exp(c_1 y + c_2)$	Power-law loss or cross-entropy loss and sigmoid activation functions
$\frac{2m-1}{2m}$ or $\frac{2m-2}{2m-1}$	$\frac{2m-2}{2m-1}$	$c_2(y + c_1)^{2m}$	Power-law loss and ReLU activation functions

Besides its theoretical significance and potential relevance in modeling critical phenomena in physical and biological systems [9, 10], the emergence of criticality is expected to play a central role in machine learning applications. Power-law distributions, in particular, enable trainable variables to explore a broader range of scales without facing exponential suppression. Consequently, criticality is presumed to prevent neural networks from becoming trapped in local minima, a highly desirable property for any learning system. However, the analysis of the learning efficiency and its relation to criticality must involve considerations of non-equilibrium systems, which is beyond the scope of the current paper. Nevertheless, we expect that the established dataset-learning duality can be developed further to shed light on non-equilibrium problems. We leave these and other related questions for future research.

Acknowledgements. The authors are grateful to Yaroslav Gusev for his invaluable assistance with both numerical and analytical problems. His expertise was crucial to the success of this project.

References

- [1] David J. Griffiths. *Introduction to Electrodynamics (3rd Edition)*. Pearson, 1999.
- [2] Richard P. Feynman, Robert B. Leighton, and Matthew Sands. *The Feynman Lectures on Physics Vol. III: Quantum Mechanics*. Basic Books, 2011.
- [3] Joseph Polchinski. *String Theory: Volume II, Superstring Theory and Beyond*. Cambridge University Press, 2005.
- [4] Vitaly Vanchurin. A quantum-classical duality and emergent space-time. *10th Mathematical Physics Meeting*, pages 347–366, March 2019.
- [5] Vitaly Vanchurin. Dual Path Integral: a non-perturbative approach to strong coupling. *European Physical Journal C*, 81:235, March 2021.
- [6] Vitaly Vanchurin. Differential equation for partition functions and a duality pseudo-forest. *Journal of Mathematical Physics*, 63:073501, July 2022.
- [7] Leonard Susskind. The world as a hologram. *Journal of Mathematical Physics*, 36(11):6377–6396, 1995.

- [8] Juan Maldacena. The Large-N Limit of Superconformal Field Theories and Supergravity. *International Journal of Theoretical Physics*, 38:1113–1133, January 1999.
- [9] Lev Davidovich Landau and E. M. Lifshitz. *Statistical physics. Pt.1.* 1969.
- [10] Artem Romanenko and Vitaly Vanchurin. Quasi-Equilibrium States and Phase Transitions in Biological Evolution. *Entropy*, 26(3):201, February 2024.
- [11] V. Vanchurin. The world as a neural network. *Entropy*, 22(11):1210, 2022.
- [12] M. Katsnelson and V. Vanchurin. Emergent quantumness in neural networks. *Foundation of Physics*, 51(94), 2021.
- [13] V. Vanchurin. Towards a theory of quantum gravity from neural networks. *Entropy*, 24(1):7, 2022.
- [14] Vitaly Vanchurin, Yuri I. Wolf, Eugene V. Koonin, and Mikhail I. Katsnelson. Thermodynamics of evolution and the origin of life. *Proceedings of the National Academy of Science*, 119(6):e2120042119, February 2022.
- [15] Vitaly Vanchurin, Yuri I. Wolf, Mikhail I. Katsnelson, and Eugene V. Koonin. Toward a theory of evolution as multilevel learning. *Proceedings of the National Academy of Science*, 119(6):e2120037119, February 2022.
- [16] M. I. Katsnelson, V. Vanchurin, and T. Westerhout. Emergent scale invariance in neural networks. *Physica A Statistical Mechanics and its Applications*, 610:128401, January 2023.
- [17] V. Vanchurin. Towards a theory of machine learning. *Mach. Learn.: Sci. Technol.*, 2(035012), 2021.
- [18] Yann LeCun, Corinna Cortes, and CJ Burges. Mnist handwritten digit database. *ATT Labs [Online]*. Available: <http://yann.lecun.com/exdb/mnist>, 2, 2010.
- [19] A.G. Ivakhnenko and V.G. Lapa. *Cybernetics and Forecasting Techniques*. Modern analytic and computational methods in science and mathematics. American Elsevier Publishing Company, 1967.
- [20] Y. Lecun, L. Bottou, Y. Bengio, and P. Haffner. Gradient-based learning applied to document recognition. *Proceedings of the IEEE*, 86(11):2278–2324, 1998.
- [21] Mark A. Kramer. Nonlinear principal component analysis using autoassociative neural networks. *AIChE Journal*, 37(2):233–243, February 1991.
- [22] Ashish Vaswani, Noam Shazeer, Niki Parmar, Jakob Uszkoreit, Llion Jones, Aidan N. Gomez, Lukasz Kaiser, and Illia Polosukhin. Attention Is All You Need. *arXiv e-prints*, page arXiv:1706.03762, June 2017.